A model for binaural response properties of inferior colliculus neurons. I. A model with interaural time difference-sensitive excitatory and inhibitory inputs

Hongmei Cai, Laurel H. Carney, and H. Steven Colburn
Department of Biomedical Engineering, Boston University, 44 Cummington Street, Boston, Massachusetts 02215

(Received 18 November 1996; revised 3 September 1997; accepted 4 September 1997)

A model was developed that simulates the binaural response properties of low-frequency inferior colliculus (IC) neurons in response to several types of stimuli. The model incorporates existing models for auditory-nerve fibers, bushy cells in the cochlear nucleus, and cells in medial superior olive (MSO). The IC model neuron receives two inputs, one excitatory from an ipsilateral MSO model cell and one inhibitory from a contralateral MSO model cell. The membrane potential of the IC model neuron (and the other model neurons) is described by Hodgkin–Huxley type equations. Responses of IC neurons are simulated for pure-tone stimuli, binaural beat stimuli, interaural phase-modulated tones, single binaural clicks, and pairs of binaural clicks. The simulation results show most of the observed properties of IC discharge patterns, including the bimodal and unimodal interaural time difference (ITD) functions, sensitivities to direction and rate of change of ITD, ITD-dependent echo suppression, and early and late inhibitions in response to clicks. This study demonstrates that these response properties can be generated by a simple model incorporating ITD-dependent excitation and inhibition from binaural neurons. [S0001-4966(98)00501-3]

PACS numbers: 43.64.Bt, 43.66.Pn [RDF]

INTRODUCTION

The inferior colliculus (IC) is a critical structure for the integration of ascending monaural and binaural pathways. It is an obligatory station for all major pathways from the lower auditory brain stem (see review by Oliver and Huerta, 1992). However, it is still not clear how these afferents interact with each other and what processing is conducted within the IC. Neural modeling of the auditory pathway is useful in providing a better understanding of the neuronal mechanisms. This study focused on the interaction of excitation and inhibition in the low-frequency region of the IC.

There have been many studies of the monaural and binaural responses of the central nucleus of the IC (Kuwada and Yin, 1983; Yin and Kuwada, 1983a, b; Kuwada *et al.*, 1984, 1987, 1989; Yin *et al.*, 1986, 1987; Carney and Yin, 1989; Spitzer and Semple, 1991, 1993; Litovsky and Yin, 1993, 1994; Yin, 1994; Fitzpatrick *et al.*, 1995). However, little modeling has been done so far with the goal of describing all available data, even though there are a few models simulating specific aspects of the data (Sujaku *et al.*, 1981; Colburn and Ibrahim, 1993; Brughera *et al.*, 1996). The lack of an inclusive model is partly due to the fact that the responses of the IC neurons show considerable variety and it is hard to describe all the data with a single model. The models of Sujaku *et al.* (1981) and Colburn and Ibrahim (1993) derive their input discharge patterns from mathematically generated patterns of action potentials simulating the discharges of monaural nuclei from each side. Another, more physiological model, such as the model of the medial superior olive (MSO) by Brughera *et al.* (1996) which simulates click responses of MSO and IC neurons, derives the input discharge patterns from bushy cell models which are in turn driven by the auditory-nerve fiber model of Carney (1993). All of these IC models restrict binaural interaction to a single neural level; hence they are unable to describe some of the data that require a hierarchy of binaural neurons to interpret.

The objective of this study was to build an explicit computational model that simulates diverse responses of cells in the IC. The modeling approach in this study has emphasized the physiological basis of the model and its components. Since an abstract model which functionally simulates the responses of neurons would constrain its physiological realism, such a generic model was not employed in this study. The IC model presented in this paper incorporates a model of auditory-nerve fibers (Carney, 1993), models of globular and spherical bushy cells (Rothman *et al.*, 1993; Joris *et al.*, 1994), and a model of MSO cells (Brughera *et al.*, 1996). The discharge patterns of each component model neuron are compatible with available physiological data. The IC neuron model is similar to the models of bushy cells and MSO cells. Specifically, it is a single-compartment neuron with a membrane specified by capacitance and conductances for several channels including voltage-sensitive (Hodgkin and Huxley, 1952) and ligand-gated excitatory and inhibitory channels (Eccles, 1964). The IC model neuron is excited by a binaural (MSO) model neuron which is sensitive to interaural time differences (ITDs) and is inhibited by another (MSO) model neuron with similar discharge properties as the excitatory binaural neuron.

The responses of IC neurons that are simulated include the responses to tone stimuli (Yin and Kuwada, 1983a), binaural beat stimuli (Yin and Kuwada, 1983a), interaural

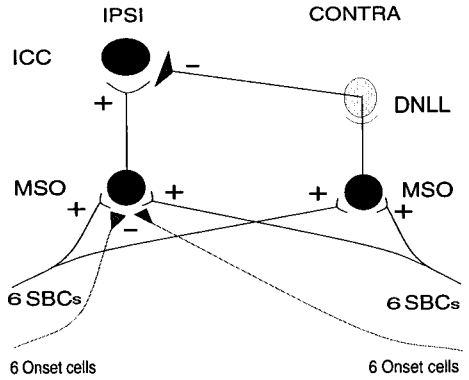

FIG. 1. Structure of the IC model, which incorporated models of peripheral structures, e.g., MSO, SBC, and AN fiber (not shown). The outlined structure of the DNLL neuron did not exist in the model but does exist anatomically. In other words, it was modeled as a relay of its input with a 1-ms delay. The SBC and onset model cells were driven by auditory-nerve fiber models. Excitatory synapses are marked by ''+'' and inhibitory synapses by ''−''.

phase-modulated stimuli (Spitzer and Semple, 1993), binaural clicks (Carney and Yin, 1989), and pairs of binaural clicks (Litovsky and Yin, 1993, 1994; Fitzpatrick *et al.*, 1995). A detailed description of these data is given where the physiological data are compared with simulation results. It will be seen that the sensitivity of IC neurons to dynamically changing ITDs cannot be described by this model. A modified IC model which has a different membrane equation and which can describe these data is presented in the accompanying paper (Cai *et al.*, 1998). In the present paper, the abilities of the simpler IC model to describe the physiological data are demonstrated.

I. METHODS

A. Description of the model

The structure of the model is based on anatomical and physiological evidence but with some simplifications. The IC model neuron is driven by an ipsilateral MSO model neuron and inhibited by a contralateral MSO model neuron via an inhibitory interneuron, presumed to be within the dorsal nucleus of the lateral lemniscus (DNLL) (Fig. 1). This structure is based on the facts that the MSO provides tonotopical projections ipsilaterally to the IC (Henkel and Spangler, 1983) and that the DNLL provides tonotopical GABAergic projections contralaterally to the IC that are presumed to be inhibitory (Adams and Mugnaini, 1984; Shneiderman *et al.*, 1988, 1993). Since the MSO projects to the DNLL ipsilaterally and tonotopically with synaptic endings associated with excitatory transmitters (Glendenning *et al.*, 1981; Henkel and Spangler, 1983), the model can be further simplified by having the contralateral MSO send inhibitory inputs directly to the IC. Although the DNLL receives many of the same inputs as the IC, to simplify the model we made the assumption that the DNLL mirrored the activity of the MSO on its ipsilateral side. Therefore the input to the IC model neuron in this study consists of two binaural neurons, one from the ipsilateral MSO and the other from the contralateral MSO. The two MSO model neurons in turn receive binaural excitatory inputs from model spherical bushy cells (SBC), which have convergent inputs from model auditory-nerve fibers.

For some simulations, the MSO model neurons also receive inhibitory inputs from onset cells, which are presumably relayed from globular bushy cells (GBCs) in the anteroventral cochlear nucleus (AVCN) via the medial nucleus of the trapezoid body (MNTB) and the lateral nucleus of the trapezoid body (LNTB) (Smith *et al.*, 1991; Cant and Hyson, 1992). The discharge patterns at each stage of the model above the auditory-nerve level are derived from the discharge times of the previous stage. Note that the inhibitory inputs from onset cells to the MSO model neuron are only relevant for the simulation of the responses to transient stimuli. Since these inhibitory inputs are assumed to be onset cells (Brughera *et al.*, 1996), the inhibition from these neurons only lasts a few milliseconds after the onset of stimulation and the presence of these cells has little influence on the responses of the model neurons one second after the onset of the stimulus, which is the beginning of the window for sustained responses to long-duration stimuli.

The bushy cells, MSO cells, and IC cells are modeled with single-compartment Hodgkin–Huxley–Eccles models (Hodgkin and Huxley, 1952; Eccles, 1964) similar to the bushy cell model in Rothman *et al.* (1993). This membrane model incorporates a nonlinear conductance as observed in bushy cells of the AVCN (Manis and Marx, 1991) and principal cells of the MSO (Smith, 1995). The primary reason for also using it for the IC cells in this study is the availability of the Rothman *et al.* (1993) model in the literature. This model accurately reproduced bushy cell membrane characteristics observed in real bushy cells by Manis and Marx (1991), Oertel (1983, 1985), and Wu and Oertel (1984). Although there is no conclusive evidence for the existence of the low-threshold potassium channels in IC neurons, nonlinear membrane characteristics associated with this channel have been observed in some IC cells (Peruzzi and Oliver, 1995). We believe that other simpler membrane models would generate essentially the same results as the Rothman *et al.* (1993) model used for the IC model neuron.

B. Auditory nerve model

The auditory nerve (AN) model of Carney (1993) was used to generate the discharge patterns of AN fibers in response to both transient and long-duration stimuli. Model parameters were the same as those used by Carney (1993). The rate function, which described the average arrival rate of the nonhomogeneous Poisson process, was slightly modified so that it closely matched the one used by Rothman *et al.* (1993). The rate function is expressed as:

$$R(t) = S(t)[1 - c_0 e^{-(t-t_l-R_A)/s_0} - c_1 e^{-(t-t_l-R_A)/s_1}] \times u(t-t_l-R_A), \quad (1)$$

where $S(t)$ is the synapse output, t_l is the time of the most recent discharge, and R_A is the absolute refractoriness of 0.75 ms. The function $u(t)$ represents the unit step function. An initial settling time of 15 ms was added to the AN model to reduce the effects of parameter initialization. Also, the time of the first action potential was set at the beginning of

the settling period rather than at the beginning of the stimulus.

C. Bushy cell model

The responses of bushy cells, including the SBCs and the GBCs, were simulated using the Rothman *et al.* (1993) model, which is based on the assumption that the soma of the bushy cell is uniform and adendritic. The model membrane contained three voltage-dependent ion channels (a fast sodium channel, a delayed-rectifierlike potassium channel, and a low-threshold potassium channel) and a voltage-independent leakage channel. The membrane potential was determined by the currents of these channels as well as those of the excitatory and inhibitory synaptic inputs. The differential equation describing the change in membrane potential V is

$$C\frac{dV}{dt}+G_B(V-E_{\mathrm{K}})+G_{\mathrm{K}}(V-E_{\mathrm{K}})+G_{\mathrm{Na}}(V-E_{\mathrm{Na}})+G_L(V-E_L)+G_I(V-E_I)+G_E(V-E_E)=I_{\mathrm{ext}}, \qquad (2)$$

where C is membrane capacitance. The conductances of the low-threshold slow potassium channel (G_B), sodium channel (G_{Na}) and delayed-rectifierlike potassium channel (G_{K}) were described by Hodgkin–Huxley-type equations as in Rothman *et al.* (1993).

The time course of the excitatory synaptic conductance was described by the following alpha function with a time constant τ_{ex} of 0.1 ms:

$$G_E(t-t_0)=G_{E_{\max}}\frac{t-t_0}{\tau_{\mathrm{ex}}}\exp\left[1-\frac{t-t_0}{\tau_{\mathrm{ex}}}\right]u(t-t_0). \qquad (3)$$

The conductance starts to increase when an input action potential arrives at time t_0 and reaches its maximum value $G_{E_{\max}}$ at time $t_0+\tau_{\mathrm{ex}}$.

The model SBCs had 25 inputs from model AN fibers with characteristic frequencies (CFs) of approximately 500 Hz. The maximum conductance of each input was 7 nS, which gave the bushy cells a primarylike peristimulus time (PST) histogram with high synchronization index to tone burst stimuli at CF (Joris *et al.*, 1994). None of the model bushy cells received inhibitory inputs.

The ''onset'' cells received inputs from 16 AN fibers with CFs evenly distributed between 350 and 650 Hz. Each input had a (subthreshold) synaptic strength of 4.0 nS. These cells showed both an onset response and a low sustained response to a tone burst. Since they were included in the model only in the simulations of the responses to transient stimuli, in which case the low sustained part of the response did not play an important role, the model was equivalent to having inhibition from onset cells when it was considered for the responses to both transient and sustained stimuli. Responses of model SBCs and onset cells are illustrated in Brughera *et al.* (1996).

D. MSO model

The MSO model neurons in this study had the same structure as the MSO model developed by Brughera *et al.* (1996), in which the differential equation for the MSO membrane potential was the same as that in the bushy cell model of Rothman *et al.* (1993) [shown in Eq. (2)]. The MSO model neurons received excitatory inputs from SBCs on both sides unless otherwise indicated. For simulations of transient stimuli, they also received inhibitory inputs from onset cells on one or both sides. The onset inhibition is presumably from GBCs in the AVCN via the nuclei of the trapezoid body; GBCs are characterized by primarylike-with-notch or onset-L responses (Smith and Rhode, 1987); both types are onset dominated. The effects of the sustained response are not explored in this study. Based on the assumption that the ventral part of the medial nucleus of the trapezoid body (MNTB) is a faithful relay of the GBCs in the AVCN, the input patterns of the MSO were taken directly from the discharge times of model SBCs and GBCs. There were four possible input types to each MSO model neuron. They were ipsilateral SBC, ipsilateral GBC, contralateral SBC, and contralateral GBC. The parameters of each input type included the number of projecting neurons, the synaptic strength, the time constant, and the delay of arrival of the input. For each of the four input types, the number of projecting neurons was six, unless otherwise indicated. The synaptic strength of the excitation was 2.5 nS, except in the simulation of responses to pairs of binaural clicks, for which the synaptic strength was 2.0 nS (which gave a sharper click ITD function). The time constant for excitation was the same as used for model bushy cells, i.e., 0.1 ms. The difference in the delay of arrival between two excitatory inputs determined the characteristic delay (CD) of the model neuron. A positive CD indicated that the excitatory inputs from the SBCs on the contralateral side of that neuron were delayed. The parameters of the inhibitory inputs were adjusted to fit different data and will be described later.

The CD of the ipsilateral MSO model neuron in our simulation was either 100 μs or zero, indicating that the model neuron was most sensitive to sounds coming from the contralateral side (when 100 μs) or the midline (when zero). The CDs of the contralateral MSO model neuron were varied for two purposes: first, to systematically study their effects on the ITD functions of the IC model neurons (in the simulation of the responses to tone stimuli) and second, to fit different properties of the physiological data (in the simulation of the responses to pairs of binaural clicks). Direct comparisons between the responses of MSO model neurons and physiological data are provided in Brughera *et al.* (1996).

E. IC model

Both linear and nonlinear current-voltage relationships have been observed in IC neurons (Peruzzi and Oliver, 1995). Due to the small number of samples, no correlation can be made between the morphology of the neurons and their current-voltage functions. There was no compelling reason as to what type of membrane equation should be used in the IC model. For simplicity, the Rothman *et al.* (1993) model was used for the IC model neuron. The differential equation describing the membrane potential was the same as that for the MSO model neurons and model bushy cells [Eq. (2)]. The excitatory synaptic conductance function was al-

ways an alpha function as described in Eq. (3), whereas the inhibitory conductance function was a linear summation of an alpha function and an exponential function, i.e.,

$$G_I(t-t_0)=\left(G_{I_{\text{input}}} \frac{t-t_0}{\tau_{\text{inh}}} \exp\left[1-\frac{t-t_0}{\tau_{\text{inh}}}\right] + 1.5G_{I_{\text{input}}} \exp\left[-\frac{t-t_0}{\tau_{\text{inh}}}\right]\right) u(t-t_0), \quad (4)$$

where $G_{I_{\text{input}}}$ is the synaptic strength of the inhibitory input. The function described in Eq. (4) ensures that the inhibition increases rapidly at onset and decays slowly, unlike the alpha function alone which builds up slowly before it reaches the peak. The rapid onset and slow decay of inhibitory postsynaptic potential have been observed in MSO cells (Smith, 1995).

The inhibitory input to the IC was always delayed by 1 ms because of the longer pathway to the IC and the extra synapse (omitted here) at the DNLL. This delay would not change the model results in any significant way (Cai, unpublished observation). The inhibitory synaptic strength and time constant of the IC were either systematically studied (in the simulations of the responses to sustained stimuli) or varied to fit the physiological data (in the simulations of the responses to transient stimuli). Detailed parameter specifications are provided in later sections.

F. Stimulus generation and simulation data analysis

Five kinds of stimuli were generated: long-duration tone stimuli, binaural beat stimuli, interaural phase-modulated stimuli, single binaural clicks, and pairs of binaural clicks. These stimuli are described in detail in later sections where the physiological data and simulation results are compared. The analyses of simulation results replicated those used in physiological experiments. All simulations were run on Silicon Graphics workstations using C under the IRIX operating system.

II. RESULTS

A. Responses to pure-tone stimuli

Responses of IC neurons to both binaural and monaural tone stimuli have been reported for physiological studies. Binaural tone stimuli are used to study the ITD functions at various stimulus frequencies, including tones at CF and off CF (Yin and Kuwada, 1983b). Monaural tone stimuli are used to study the phase locking of neurons (Kuwada *et al.*, 1984). In this section, simulations of these binaural and monaural response properties related to tone stimuli are presented.

1. Tone ITD functions

The ITD function describes the relationship between response rate and interaural time difference. The ITD functions from MSO neurons obtained from tone stimulus are usually approximately sinusoidal with a frequency equal to stimulus frequency (Yin and Chan, 1990; Goldberg and Brown, 1969). The tone ITD functions from IC neurons, however, show wide variations in shape. Yin and Kuwada (1983a) gave some examples of the interaural phase difference (IPD) functions of IC neurons in response to tone stimuli (their Fig. 3). Some of the IPD functions have a single peak in one cycle, while some others show a bimodal shape. Bimodal IPD functions have not been observed in MSO neurons.

Figure 2 shows the IPD function of some IC model neurons. The tone stimuli in our simulations were 65-dB sine waves with a duration of three seconds. The frequency of the tone was 500 Hz. For each ITD, only one sweep of the stimulus was presented and the response rate was calculated from the number of discharges during the last two seconds of the stimulus. The range of ITDs, from -2 to $+2$ ms with steps of 0.1 ms, represented two cycles of the ITD function for a tone frequency of 500 Hz. The IPD function was obtained by averaging the ITD functions over both cycles and converting the horizontal axis from time to phase.

The model parameters for tone stimuli, including ipsilateral and contralateral MSO and IC model neurons, are listed in Table I. The synaptic strength and time constant of the inhibitory input to the IC were systematically varied. Three combinations of these two parameters representing weak, moderate, and strong inhibition are listed in Table II. The excitatory synaptic strength from the ipsilateral MSO model neuron to the IC model neuron was chosen such that an input discharge from the ipsilateral MSO would generate an output discharge in the IC over the full range of its discharge rates in the ITD function, when inhibition was absent. The CD of the ipsilateral MSO neuron was 100 μs, and the CD of the contralateral MSO neuron was set at four different values: -60, 50, 150, and 400 μs. These values were chosen based on the fact that most (93%) of the CDs of MSO neurons in a cat are distributed between 0 and $+400$ μs, corresponding to stimuli in the contralateral sound field (Yin and Chan, 1990). Very few MSO neurons respond preferentially to sound coming from the ipsilateral side, corresponding to a negative CD.

The four panels of Fig. 2 correspond to four different CDs of the contralateral MSO model neuron. For each CD, in the case of weak inhibition (solid curve), the IPD function of the IC model neuron was almost the same as that of the ipsilateral MSO. The inhibition from the contralateral MSO was not strong enough to affect the ITD sensitivity of the IC. When the inhibition became stronger, however, the contralateral inhibition reshaped the IPD function of the IC. The response rate of the IC model neuron at a certain ITD depended on the interaction of the excitation and the inhibition. Note that the relation between the output response rate and the excitatory and inhibitory input rates of the IC was nonlinear. The peak of the ITD function was more likely to be affected by inhibition than the trough, because at a high response rate the interspike interval of the input firing was short. An inhibitory conductance change during a short period of time might be sufficiently long to inhibit the neuronal discharge at the time of the next excitatory input firing. The lower the excitatory input discharge rate, the less it would be affected by the inhibition.

The CD of the contralateral MSO affected the ITD-tuning of the IC such that excitations interacted with different levels of inhibition over the IPD range, and therefore

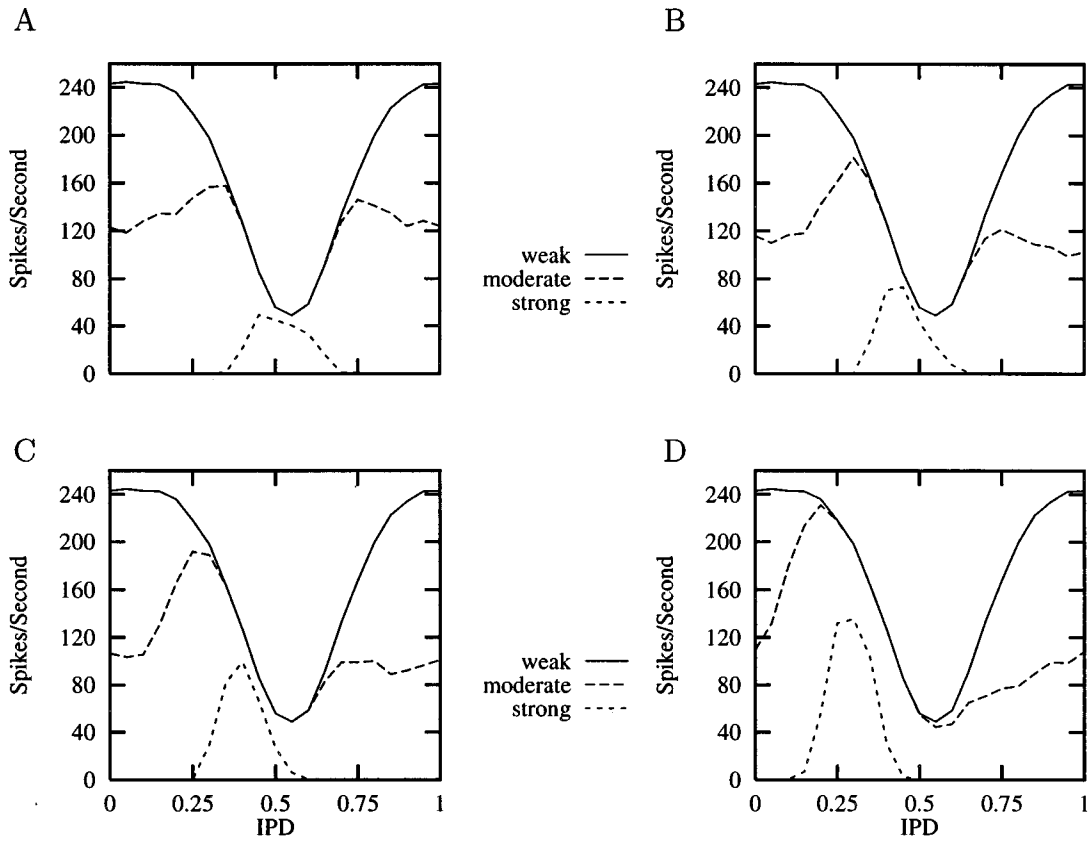

FIG. 2. IPD functions of IC model neurons when the inhibitions to the IC were ''weak,'' ''moderate,'' and ''strong.'' The three IPD functions in each panel from top to bottom represent ''weak'' (solid), ''moderate'' (long dashes), and ''strong'' (short dashes) inhibition. The CDs of the contralateral MSO model neuron were: -60 μs (A), 50 μs (B), 150 μs (C), and 400 μs (D). Input parameters of the IC model neurons are given in Tables I and II.

influenced the shape of the IPD function of IC. A given set of parameters, e.g., those for moderate inhibition, may result in either single-peaked [contralateral CD of 150 and 400 μs, Fig. 2(C) and (D)] or double-peaked [contralateral CD of -60 and 50 μs, Fig. 2(A) and (B)] IPD functions.

2. Changing stimulus frequency

The effects of stimulus frequency on the ITD functions of IC neurons have been studied physiologically by Yin and Kuwada (1983b). They plotted the ITD functions at different frequencies on a common axis and found that for some cells the ITD functions showed peaks or troughs at a common CD. The ITD functions of the IC model neurons at three frequencies, i.e., 400, 500, and 600 Hz, were simulated with stimulus intensity and duration the same as those in previous simulations. Figure 3 shows the ITD functions of the ipsilateral MSO and IC model neurons at the three frequencies. The CD of the ipsilateral MSO was 100 μs, whereas that of the contralateral MSO was 50 μs. Each ITD function of the ipsilateral MSO model neuron [Fig. 3(A)] was a sinusoidlike function with a frequency equal to stimulus frequency. By visual inspection, these curves showed a common peak at the CD of the model neuron, which was 100 μs. The relationship between the mean interaural phase of the response and the stimulus frequency was linear. The ITD functions of the IC model neuron with weak inhibition showed a similar prop-

TABLE I. Model parameters for tone stimuli. The two MSO model neurons receive only excitatory inputs. The ''C'' or ''I'' indicates that the inputs come from the contralateral side (''C'') or the ipsilateral side (''I'') with respect to the neuron that receives the inputs. The dash, —, represents ''not applicable.''

Parameters	Ipsilateral MSO exc	Contralateral MSO exc	IC exc	IC inh
Number of projecting neurons	6(C,I)	6(C,I)	1(I)	1 (C)
Synaptic strength (nS)	2.5	2.5	25	varied[a]
Time constant (ms)	0.1	0.1	0.1	varied[a]
CD of MSO (μs)	100	50[b]	—	—
Delay of arrival (ms)	0	0	0	1

[a]The parameter values are given in Table II.
[b]Note that the CD of the contralateral MSO cell was systematically varied in the simulation of the responses to 500-Hz tone stimuli.

TABLE II. Inhibitory input parameters to the IC in the cases of ''weak,'' ''moderate,'' and ''strong'' inhibition.

	Weak	Moderate	Strong
Synaptic strength	6 nS	8 nS	10 nS
Time constant	2 ms	3.5 ms	10 ms

erty, although the peak of the ITD function at 400 Hz was affected. The ITD functions of the IC model neurons with moderate and strong inhibition, however, did not have a peak at a common ITD. In fact, with strong inhibition, the ITD functions have a common minimum and appear similar to the response of excitatory-inhibitory cells in the LSO (Kuwada *et al.*, 1997). It was also found that an ITD function with a single peak for some frequencies may be bimodal for some other frequencies, such as the IC model neuron with moderate inhibition. The ITD function of this model neuron was unimodal at 600 Hz, whereas the ITD functions were bimodal at 500 and 400 Hz.

3. Phase locking to monaural stimuli

The phase locking of IC model neurons in response to 500-Hz monaural tone stimuli was characterized by the synchronization index (Johnson, 1980). The period histogram of the responses during the last 2 s of the 3-s stimulus duration was used for these calculations. The significance of the synchronization index was evaluated by the Rayleigh criterion (Mardia, 1972), which tests whether the histogram was a sample of a uniform distribution. If for a histogram, $2nR^2 > 13.8$, where n is the number of discharges and R is the synchronization index, the probability that the histogram is a sample of a uniform distribution is 0.001.

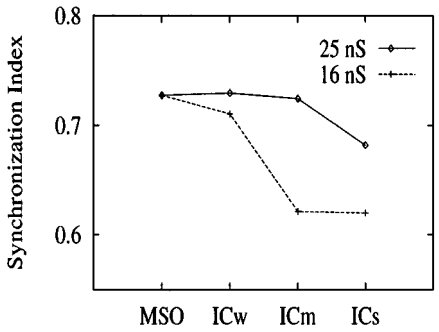

FIG. 4. Synchronization index of ipsilateral MSO and IC model neurons with different inhibitions. The excitatory synaptic strengths were 25 and 16 nS. The IC model neurons with weak, moderate, and strong inhibition are represented by ICw, ICm, and ICs, respectively. The CD of the ipsilateral MSO was 100 μs, whereas that of the contralateral MSO was 50 μs. Parameters of the IC model neurons are given in Tables I and II. The synchronization index was the average of those obtained from monaural stimuli to each side. The stimulus was a 500-Hz monaural tone with a duration of 3 s.

The synchronization indices obtained from monaural stimulation of each side were averaged. Figure 4 shows the mean synchronization index for the ipsilateral MSO model neuron and for IC model neurons with weak, moderate, and strong inhibition. For these model neurons, the CD of the

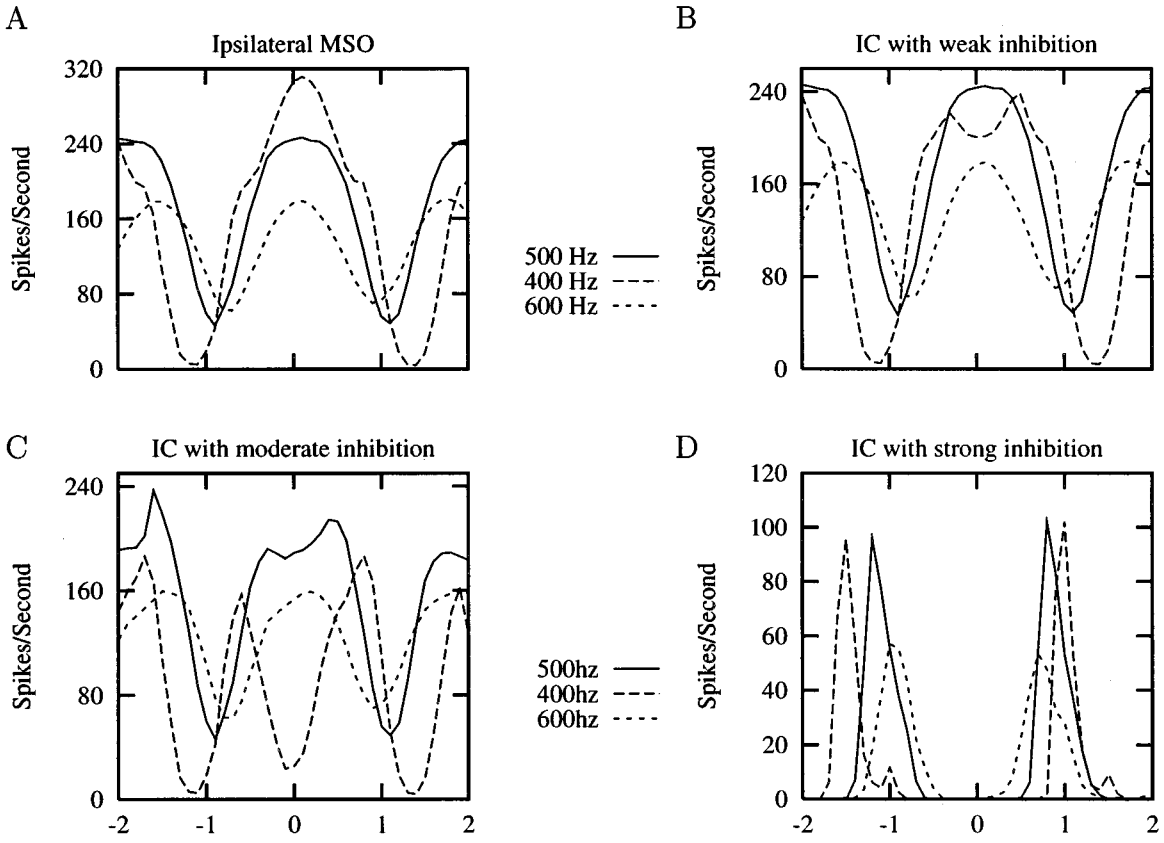

FIG. 3. Frequency dependence of ITD functions of ipsilateral MSO and IC model neurons with different strengths of inhibition. The CD of the ipsilateral MSO was 100 μs, whereas that of the contralateral MSO was 50 μs. Input parameters of the IC model neurons are given in Tables I and II.

ipsilateral MSO was 100 μs and that of the contralateral MSO was 50 μs. Two values of the excitatory synaptic strength were studied, i.e., 25 and 16 nS. The synchronization index of the IC model neuron was slightly lower than that of the ipsilateral MSO model neuron in each case. Weaker excitation (16 nS) resulted in a larger decrease in synchronization index. Physiological data show that most, if not all, MSO neurons show phase locking (Yin and Chan, 1990); however, only a small number of low-frequency IC neurons phase lock to monaural stimuli (18% in Kuwada *et al.*, 1984). For those which do phase lock, the synchronization index is low. The model failed in simulating these physiological responses.

B. Responses to binaural beat stimuli

For the tonal stimuli described above, the IPD is constant over the duration of the stimulus. The IPD function obtained from the tone responses is thus referred to as the static IPD function. For other types of tonal stimuli, such as the binaural beat stimuli, the IPD dynamically changes over the time course of the stimuli. The IPD function converted from the PST histograms in response to such stimuli is referred to as the dynamic IPD function. In this section, the responses of IC model neurons to binaural beat stimuli are reported.

The binaural beat stimulus involves two tones with slightly different frequencies presented simultaneously and separately to the two ears. The larger the difference, or beat frequency, the faster the IPD changes over time. The sign of the beat frequency determines the direction of motion of the perceived sound. Our convention is that a positive beat frequency indicates that the higher-frequency tone is delivered to the contralateral ear. A comparison between dynamic and static IPD functions has been provided by Yin and Kuwada (1983a); the dynamic functions are sharper than the static ones (their Fig. 3). Note that the dynamic functions go to zero at some troughs while the static ones do not. Even though these functions are normalized to their maximum response rates, normalization does not affect zero rate.

In our simulations, the frequencies of the tones delivered to the two sides were 500 and 501 Hz (beat frequency $=\pm 1$ Hz), unless otherwise indicated. The duration of the stimulus was 8 s, repeated every 8.5 s for five presentations. The PST histograms during the last 7 s of the stimulus were averaged to get the dynamic IPD functions. The parameters of the IC model were identical to those used in the simulation of the responses to tone stimuli (Table I) with the CD of the contralateral MSO model neuron fixed at 50 μs.

Binaural beat stimuli were presented in both directions for each simulation. Figure 5 shows the result of the same three model neurons as in Fig. 2(B). The dynamic IPD functions obtained from the binaural beat stimulus (shown as bars) are plotted along with the static IPD functions from tones (solid curves). The left column shows the responses in one direction (positive beat frequency) and the right column shows those in the opposite direction (negative beat frequency). For these three inhibitory levels, no matter what the shapes of IPD functions were [unimodal as in Fig. 5(A), (B), (E), and (F), or bimodal as in Fig. 5(C) and (D)], the dynamic and static IPD functions were always consistent or overlapping.

Most IC neurons have approximately the same response to the two directions of dynamic phase change (like the above model neurons). However, a small number of cells in the IC exhibited sensitivity to the sign of the beat frequency (Yin and Kuwada, 1983a). In addition, there were some other cells sensitive to the absolute value of the beat frequency or the rate of interaural phase change (Yin and Kuwada, 1983a). The IC model with a long inhibitory time constant was capable of describing this phenomenon. A long time constant for the inhibition had an effect similar to a low-pass filter, which made it possible for excitatory input at one moment to interact with inhibitory input at a previous time. The long-lasting inhibition resulted in a shift of the maximum inhibition in the PST histogram. Therefore the maximum inhibition occurred at different IPDs for different directions or rates of the binaural beat stimuli. For a dynamic phase change in one direction, if the strong inhibition coincided with strong excitation, the response of the IC neuron was weak at some IPDs. If in the other direction, strong inhibition happened to coincide with weak excitation, the IC cell still received strong excitation during part of the cycle and responded vigorously at the same IPDs. Therefore the model IC neuron responded differently to different directions of the binaural beat stimuli at a given interaural phase.

A model neuron was simulated with a long inhibitory time constant, relative to that of the model neurons in Fig. 5. The detailed parameters are listed in Table III. The inhibitory synaptic strength was kept at 6 nS, as in the ''weak inhibition'' case. The time constant of inhibition was 30 ms. The excitatory synaptic strength to the IC was increased from 25 to 40 nS to obtain a reasonable response rate at a favorable beat frequency.

Figure 6 shows the responses of this model neuron to a 1-Hz binaural beat stimulus and to a 5-Hz beat stimulus in both directions. The neuron showed a stronger response to the 1-Hz beat than to the 5-Hz beat. When the binaural beat frequency was 5 Hz, both excitatory and inhibitory input firings were repeated every 200 ms. Since the inhibition had a long time constant, inhibition built up from cycle to cycle but excitation did not. The neuron did not catch up with the dynamic IPD change and consequently responded very weakly. If the inhibition were not so strong, a stronger response to the 5-Hz binaural-beat stimulus would have been seen. In response to the 1-Hz beat frequency, the model neuron responded better to the motion of sound in the direction toward the ipsilateral ear (negative beat frequency).

The current model could only simulate neurons that respond more vigorously to slower binaural beats than to faster beats. However, some IC cells show the opposite property (Yin and Kuwada, 1983a). Other processes must be involved in those neurons.

C. Response to interaural phase-modulated stimuli

The interaural phase-modulated (IPM) stimulus is another type of tonal stimuli in which the IPD is varying over the duration of stimuli. It is different from the binaural beat

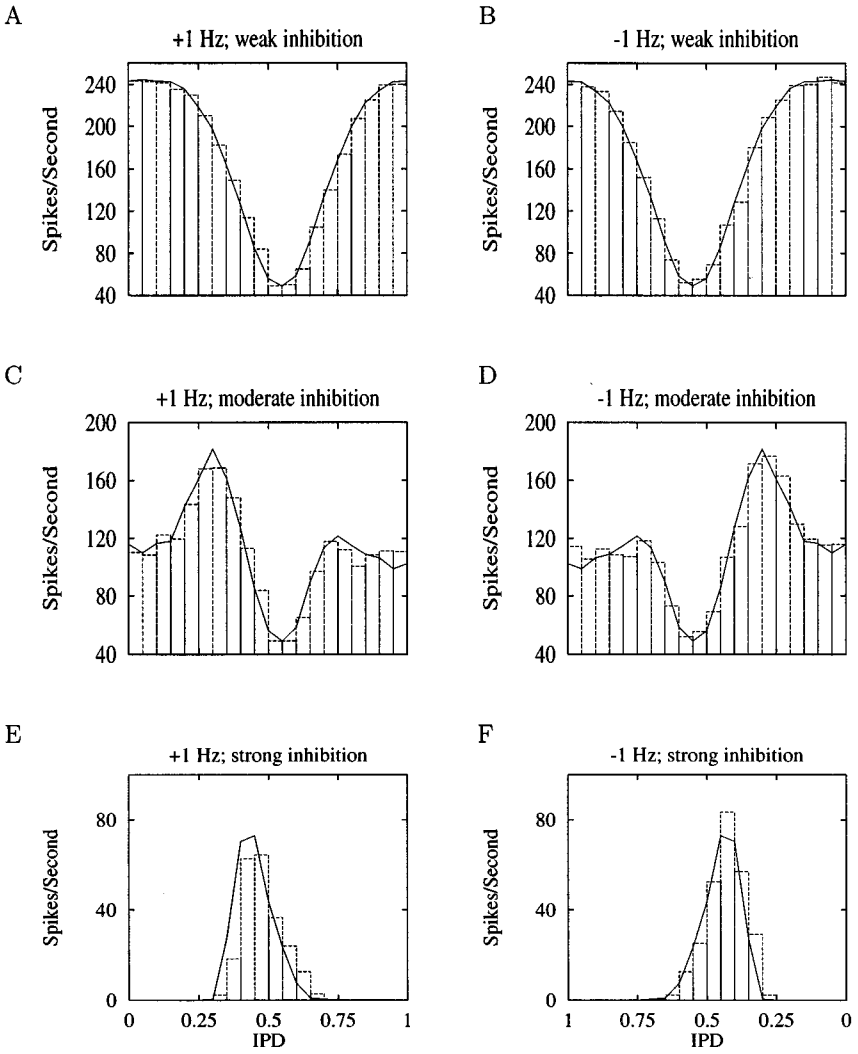

FIG. 5. Dynamic IPD functions (bars) of IC model neurons obtained from binaural beat stimuli along with the static IPD functions (solid curves) obtained from tone stimuli. The beat frequency and the inhibition level to the IC are shown at the top of each panel. Parameters of the IC model neurons are given in Tables I and II.

stimulus in that two tones of the same average frequency are delivered to the two ears. However, the phase of one of the sine waves is modulated by a triangular wave. When a constant phase offset is included in one of the tone waveforms, the direction, the range, and the center position of the apparent sound movement can be manipulated.

Spitzer and Semple (1993) used triangular interaural phase-modulated tones in studies of IC cells in anesthetized cats and gerbils. The static IPD functions of IC neurons were compared with the IPD arcs obtained from IPM stimuli over partially overlapping IPD ranges. The majority of units (about 94%) showed a systematic relationship between the

TABLE III. Parameters of the IC model neuron simulating directional sensitive neurons for binaural beat stimuli. The two MSO model neurons receive only excitatory inputs. The ''C'' or ''I'' represents that the inputs come from contralateral side (''C'') or ipsilateral side (''I'') with respect to the neuron that receives the inputs. The dash, —, represents ''not applicable.'' Parameter values chosen specifically for this simulation are shown in italics.

Parameters	Ipsilateral MSO exc	Contralateral MSO exc	IC exc	IC inh
Number of projecting neurons	6(C,I)	6(C,I)	1(I)	1(C)
Synaptic strength (nS)	2.5	2.5	*40*	*6*
Time constant (ms)	0.1	0.1	0.1	*30*
CD of MSO (μs)	100	50	—	—
Delay of arrival (ms)	0	0	0	1

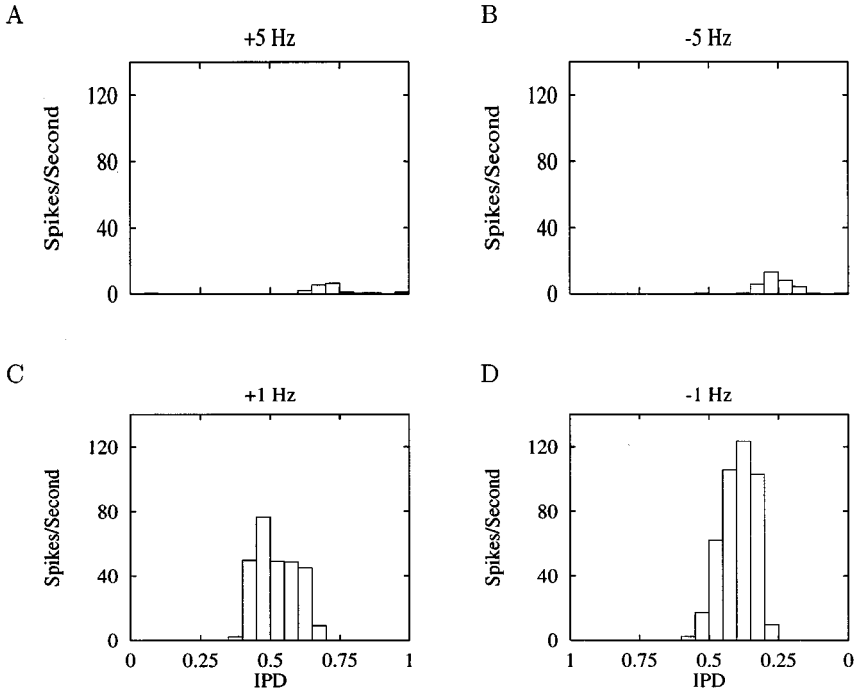

FIG. 6. IPD functions of a direction- and rate-sensitive IC model neuron. The model neuron responded more vigorously when the rate of binaural beat was slow and/or when the direction of the beat was towards the ipsilateral ear (negative beat frequencies). Parameters of the IC model neurons are given in Table III.

IPD function obtained from IPM and that from pure tones. Motion of IPD toward the peak of the function is associated with increased discharge probability and motion toward the trough is associated with decreased discharge probability. Within each IPD range, the IPD function is consistently sharpened by the dynamics of IPD (cf. their Fig. 8).

Binaural tones of 65 dB SPL with triangular modulated interaural phase were applied in the simulation. The carrier frequency of both tones was set to the CF of the model neuron, i.e., 500 Hz. The modulation frequency was 2 Hz and the modulation depth was 90° such that the phase changed at the same rate as for a binaural beat stimulus with a beat frequency of 1 Hz. The duration of the stimulus was 10 s, and it was repeated four times. The PST histograms of the last 9 s were averaged and converted to an IPD function.

Figure 7 shows the IPD functions of three model neurons, with ''weak,'' ''moderate,'' and ''strong'' inhibition, in response to IPM stimuli (dashed curves) and constant-phase tones (solid curves). The parameters of the model neurons are given in Table I. Arrows on the top of each curve indicate the range and direction of the IPD change. Each panel shows the profiles for half the cycle of IPD, i.e., the IPD change in one direction. Curves on the left column correspond to increasing IPD, while those on the right correspond to decreasing IPD. In contrast to the physiological data obtained by Spitzer and Semple (1993), the response profiles for overlapping IPDs were continuous in both directions. The IPD arcs could be superimposed to form a continuous IPD function, which resembled the static function. A very small shift of the dynamic IPD functions toward the direction of IPD variation was associated with the latency of the responses of IC neurons. The shift observed in the bottom panels was also contributed by the long time constant of inhibitory input in addition to the latency. Except for the shift, the response profiles of IPM stimuli and the static-phase tones were identical. Although the IPD profiles for both directions were not plotted on a common axis, they were still comparable since they all followed the static function, which was the same for both directions. When these IPD profiles were plotted with the IPD functions obtained from the binaural beat stimuli at a beat frequency of 1 Hz (not shown), it was clear that these functions were perfectly overlapping.

In the above sections, the simulation results of the responses of IC model neurons to long-duration tonal stimuli were demonstrated. In the following sections, the responses of IC model neurons to transient stimuli will be described, including single binaural clicks and pairs of binaural clicks.

D. Responses to single binaural clicks

The responses of IC neurons to clicks with interaural delays were studied by Carney and Yin (1989). Simulations are presented below for comparison to the neuron of which the responses are shown in Fig. 8. Although ipsilaterally driven neurons such as this one are not the major types of neurons in the IC, this neuron possesses some features common to the click responses of many IC neurons: sensitivity to short ITDs; late, long-lasting inhibitions; and early, short-lasting inhibitions (Carney and Yin, 1989).

To model this particular neuron, the structure of IC models in this study (Fig. 1) was simplified in two ways. First, the ipsilateral MSO neuron received inhibitory input only from the contralateral onset cells. This unbalanced in-

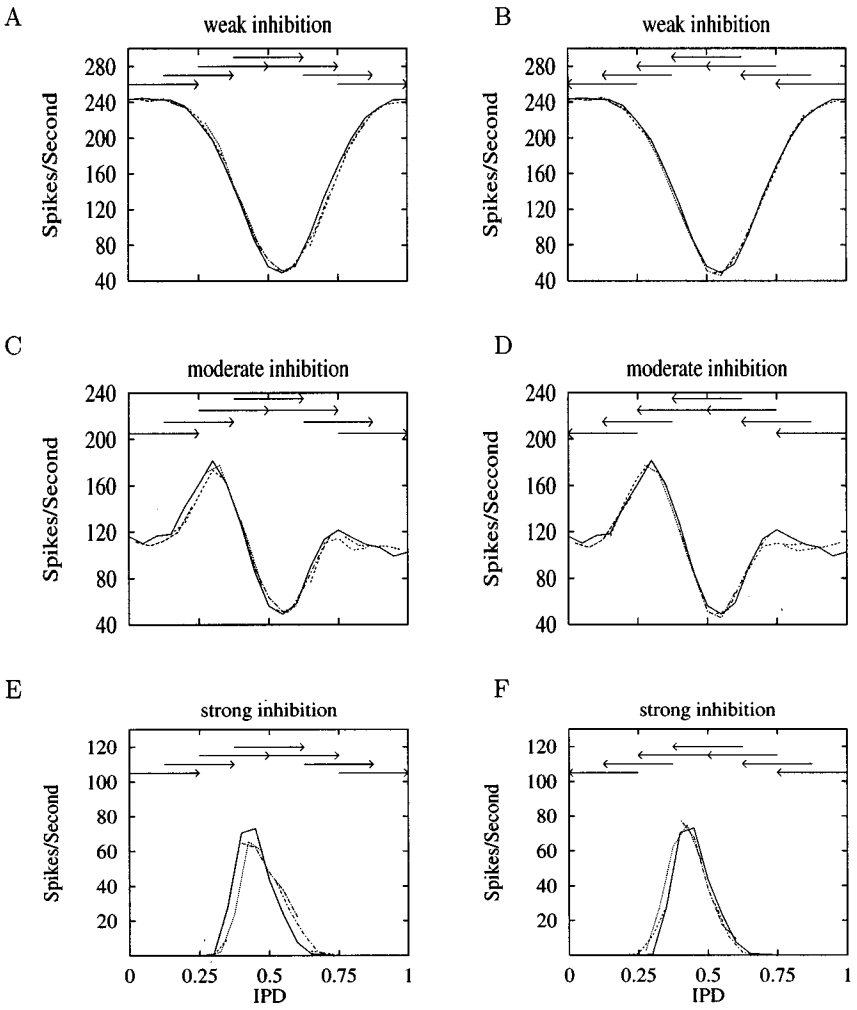

FIG. 7. Comparison of the IPD functions of three model neurons with ''weak inhibition'' [(A) and (B)], ''moderate inhibition'' [(C) and (D)], and ''strong inhibition'' [(E) and (F)], obtained from IPM stimuli (dashed curves). The solid curves are the static IPD functions obtained from 3-s tone stimuli. Arrows on the top show the range and direction of IPD change in IPM stimuli. The rate of IPD change was 360°/s. Parameters of the IC model neurons are given in Tables I and II.

hibition resulted in the asymmetric monaural responses of the MSO model neuron itself and hence the IC model neuron. Second, the contralateral MSO model neuron received excitation only from the SBCs on its ipsilateral side. In this case, only the contralateral stimulus (with respect to the IC model neuron) could trigger the contralateral MSO and hence caused the long-lasting inhibition to the IC. Empirically, about 18% of MSO neurons have been observed as monaural cells (Yin and Chan, 1990). Note that the asymmetry in model structure was required for some cells such as the one in Fig. 8. For other cells which showed approximately symmetric responses, a symmetric structure, which includes all pathways in Fig. 1, could be used. A model neuron with no inputs from one side is an extreme case of weak inputs from that side.

The parameters used for this model neuron are listed in Table IV. The excitatory input parameters to the two MSO model neurons were identical to those of the previous simulation, except that the contralateral MSO model neuron received excitatory inputs only from its ipsilateral side. It was assumed that the inhibitory inputs are relayed from GBCs in the AVCN via the nuclei of the trapezoid body (Smith *et al.*, 1991; Cant and Hyson, 1992). GBCs have thicker axons than SBCs and the synaptic connections between GBCs and cells in MNTB are secure (Finlayson and Caspary, 1989). Therefore it is possible that the contralateral inhibitory inputs arrive earlier than those from the SBCs. For the ipsilateral MSO model neuron, inhibitory inputs arrived 3 ms earlier than the excitatory inputs from both sides. The value of 3 ms was chosen based on the observation (Carney and Yin, 1989) that at small negative ITDs, the response to the leading (ipsilateral monaural) click is suppressed by the lagging (contralateral monaural) click when the ITD is as large as -2.8 ms (Fig. 8). The synaptic strength and time constant of the inhibition to the IC were 40 nS and 5 ms, respectively.

The click stimulus used in this study was a 100-μs pulse. The intensity of the binaural clicks was 55 dB peak-equivalent SPL, unless otherwise indicated. Fifty repetitions of single binaural click stimuli were presented every 150 ms. The range of interaural time differences, or the delay between the two monaural clicks, was extended from -10 ms to 30 ms.

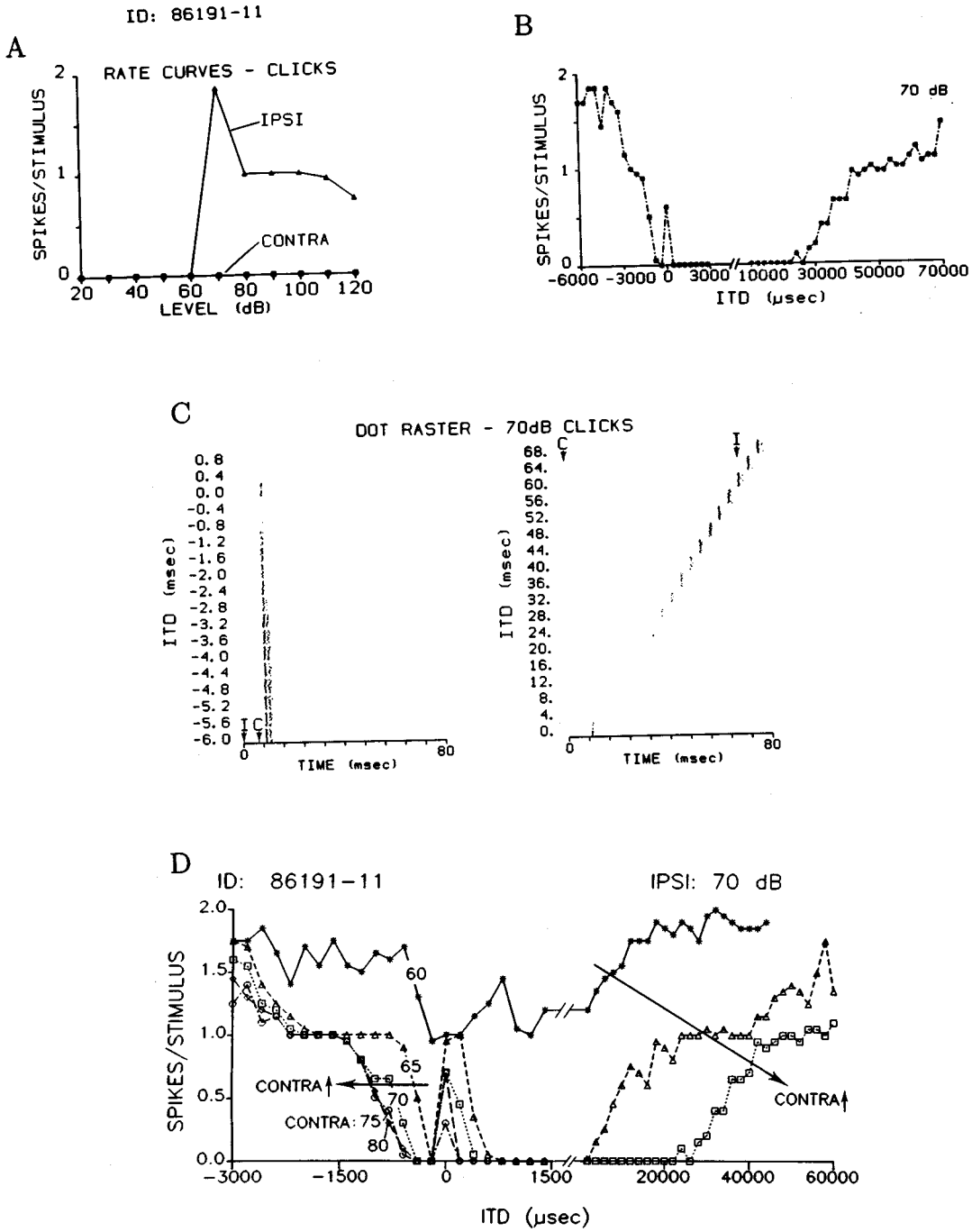

FIG. 8. Response of an IC neuron with early and late inhibition. Estimated best frequency was 2.8 kHz. (A) Rate-level curves of monaural clicks. (B) Click ITD function at 70 dB. (C) Dot rasters for responses to 70-dB clicks with varied ITDs. (D) Click ITD functions at various contralateral intensities when ipsilateral intensity was fixed at 70 dB. [From Carney and Yin (1989), their Figs. 6C, D, E and Fig. 8C. Reprinted with permission.]

1. Rate-level curves

The rate-level curves of the model neuron for monaural click stimuli are plotted in Fig. 9(A). The IC model neuron did not respond to contralateral stimuli except at low levels. At a high level, since the inhibition from the contralateral onset cells arrived earlier at the ipsilateral MSO model neuron than the excitation from the SBCs, the ipsilateral MSO model neuron and hence the IC model neuron did not respond to the stimulus. At levels lower than 45 dB, the inhibition to the ipsilateral MSO model neuron from the contralateral onset cells was not strong enough to suppress the excitation driven by both the spontaneous response of ipsilateral SBCs and the stimulus-evoked response of the contralateral SBCs. For ipsilateral monaural stimuli, the response rate increased monotonically when the intensity of the stimulus was increased up to 75 dB. The model IC neuron responded to ipsilateral stimuli because the inhibition from the onset cells was too weak to suppress the response of the ipsilateral MSO model neuron. The slight decrease of response rate at 90 and 105 dB was due to the ringing of model auditory-nerve fibers, which reduced the synchronization of the first spike in the response (Cai, 1997).

TABLE IV. Parameters of the IC model neuron simulating click response of neuron ID 86191-11 in Carney and Yin (1989) (also shown in Fig. 8). The parameters that are different from Table I are represented in italics. ''C'' represents input from the contralateral side of a certain neuron, and ''I'' represents input from the ipsilateral side of a neuron.

Parameters	Ipsilateral MSO		Contralateral MSO	IC	
	exc	inh	exc	exc	inh
Number of projecting neurons	6(C,I)	6(C)	6(I)	1(I)	1(C)
Synaptic strength (nS)	2.5	*3.0*	2.5	25	*40*
Time constant (ms)	0.1	*2*	0.1	0.1	5
CD of MSO (μs)	0		—	—	—
Delay of arrival (ms)	0	*−3*	0	0	1

2. ITD functions

The ITD function of this model neuron for ipsilateral and contralateral clicks at 55 dB SPL is shown in Fig. 9(B) (solid curve). When the clicks from the two sides were presented simultaneously (zero ITD), the model neuron responded with 1 spike/stimulus. The model neuron demonstrated ITD sensitivity at small ITDs. When the stimulus to the contralateral side was delivered shortly after the stimulus to the ipsilateral side (ITDs around −2 ms), the response of the model neuron to the ipsilateral stimulus was suppressed due to the early inhibition to the ipsilateral MSO model neuron. For large ITDs in either direction, the neuron responded to each click separately. Since the model neuron did not respond to the contralateral monaural click at 55 dB, the discharge probability at large ITDs was the same as that to the ipsilateral click alone, which was about 0.9.

A comparison of the ITD function of the IC model neuron with that of the ipsilateral MSO cell (Cai, 1997) indicated that the low discharge rates of the IC model neuron at ITDs between 2 and 11 ms were caused by the inhibition from the contralateral MSO neuron. At these ITDs, the response of the IC model was remarkably suppressed. The MSO model cell, however, showed a clear cyclic dependence of response rate on ITD with a frequency equal to the CF (500 Hz) and the peak response probabilities between 1 and 0.8. The trough rates increased with ITD until they reached

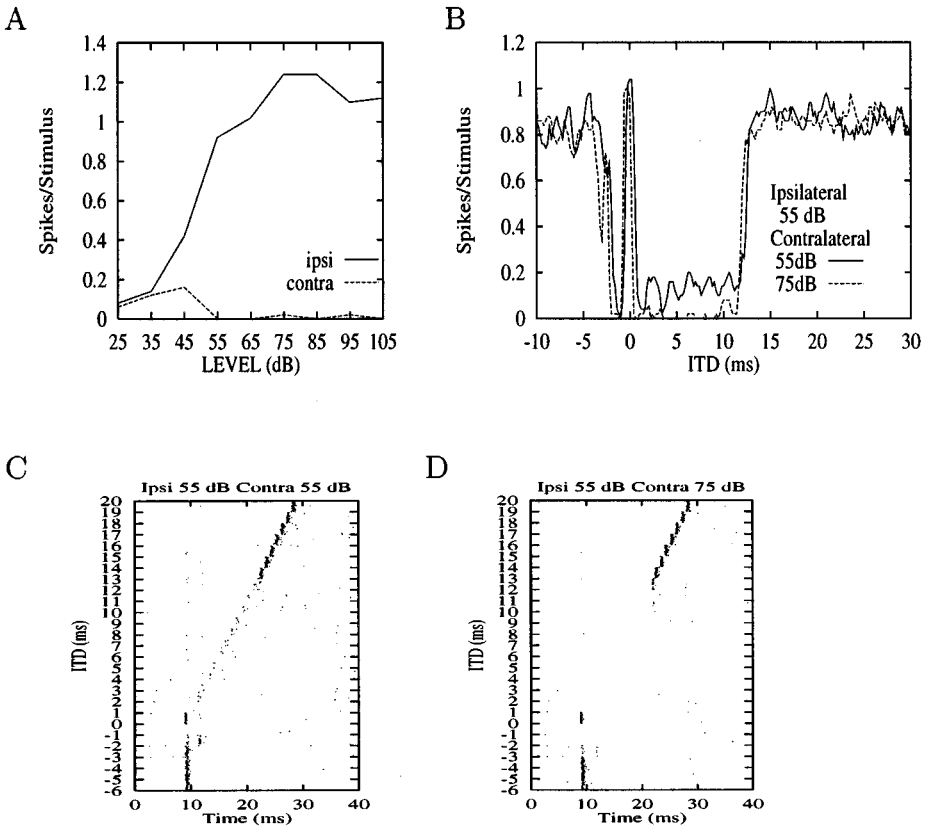

FIG. 9. Response of the IC model neuron simulating click responses of neuron ID 86191-11 (Carney and Yin, 1989) shown in Fig. 8. (A) Rate-level curves of monaural responses. (B) Click ITD functions of IC model neuron for two contralateral stimulus levels. Solid curve: ipsilateral 55 dB SPL and contralateral 55 dB SPL. Dashed curve: ipsilateral 55 dB SPL and contralateral 75 dB SPL. (C) and (D) dot-raster plots of the responses for ITDs between −6 and 19 ms with 1-ms steps. Ipsilateral stimulus intensity was 55 dB in both plots. Contralateral stimulus intensity was 55 dB in (C) and 75 dB in (D). Parameters of the IC model neuron are given in Table IV.

TABLE V. Parameters of an IC model neuron simulating ITD-dependent echo suppression. This neuron showed stronger suppression when the leading click had an ITD that elicited a strong response. Parameters shown in italics are those critical for the simulation of data. The dash, —, represents ''not applicable.''

Parameters	Ipsilateral MSO		Contralateral MSO		IC	
	exc	inh	exc	inh	exc	inh
Number of projecting neurons	6(C,I)	6(C,I)	6(C,I)	6(C,I)	1(I)	1(C)
Synaptic strength (nS)	2.0	7.0	2.0	4	25	*30*
Time constant (ms)	0.1	4	0.1	2	0.1	*20*
CD of MSO (μs)	0		*0*		—	—
Delay of arrival (ms)	0	0	0	0	0	1

around 0.9. The peaks of the MSO response rate were seen in the response of the IC model cell, since the inhibition at this stimulus intensity was not strong enough to overcome the excitation from the ipsilateral MSO.

The dot-raster plot of the responses of the IC model neuron [shown in Fig. 9(C)] shows the discharge times at ITDs between -6 and 19 ms for an integer step of 1 ms. This plot basically indicates the same things as the ITD function shown in Fig. 9(B). The early inhibition was indicated by the absence of responses at an ITD of -1 ms. The late inhibition was indicated by the weak response (fewer dots) at ITDs between 1 and 12 ms.

3. Changing contralateral stimulus level

The effects of stimulus intensity on the ITD function of IC neurons were studied both in physiological data (Carney and Yin, 1989) [reprinted in Fig. 8(D)] and in simulation [Fig. 9(B), dashed curve]. In the simulation, the ipsilateral level was fixed at 55 dB SPL while the contralateral level was either 55 dB or 75 dB SPL.

Note that the dashed ITD function was shifted to the left of the solid curve and its peak near zero ITD was narrower. When the stimulus intensity was higher, the first action potentials of the SBCs were evoked with a shorter latency. The effect was similar to having a more positive ITD. The narrowness of the peak near zero ITD was caused by the higher synchronization of the first action potentials at 75 dB SPL. Since the probability of discharge of the contralateral MSO model neuron was larger when the stimulus intensity was higher, a stronger suppression was observed at large ITDs in the 75-dB case. However, it was interesting to note that the duration of the suppression was not so prolonged as was observed in the physiological data (cf. Fig. 8). Also, the recovery of the lagging response was not gradual as in the physiological data. Two factors contributed to these observations. First, there was only *one* inhibitory input to the model IC neuron and the maximum number of inhibitory spikes triggered by each click was *one*, so the time of arrival and the strength of the inhibition was approximately the same in both levels, except for a small latency shift caused by the difference in intensity. Second, the inhibitory conductance function was a deterministic function driven by each inhibitory input action potential. The dot raster of the response in the 75-dB case is shown in Fig. 9(D). A comparison between the dot raster plots in Fig. 9(C) and (D) indicated that the late inhibition was stronger in the 75-dB case because of the complete lack of responses at ITDs between 1 and 10 ms.

E. Responses to pairs of binaural clicks

The responses of IC cells to pairs of dichotic clicks that mimic the stimulus used to observe the precedence effect have been studied in physiological experiments. The precedence effect, sometimes called the law of the first wavefront, refers to the psychophysical observation that the first stimulus in a pair of stimuli dominates the perceived location of the pair, when the pair is closely spaced in time (Blauert, 1983). Recent physiological studies have explored this phenomenon by using pairs of binaural click stimuli (Litovsky and Yin, 1993, 1994; Fitzpatrick *et al.*, 1995). When a pair of binaural clicks is presented to the two ears with a short interclick delay (ICD), the response of an IC neuron to the lagging stimulus is suppressed. When the ICD is increased, the response to the lagging stimulus recovers (Litovsky and Yin, 1993, 1994; Fitzpatrick *et al.*, 1995). The amount of suppression depends on the ITD of the leading stimulus. In some neurons, a leading stimulus with an ITD that evokes a strong response (referred to as strong ITD) has stronger suppressive effect than that with an ITD that evokes a weak response (referred to as weak ITD); in other neurons, a leading stimulus with a weak ITD has a stronger suppressive effect than a leading stimulus with a strong ITD (Litovsky and Yin, 1993, 1994; Fitzpatrick *et al.*, 1995).

Responses to 20 repetitions of pairs of binaural clicks were simulated with 150 ms between each pair. The range of ICDs was between 1 and 70 ms. The technique used to count the number of discharges in response to the leading and lagging clicks was the same as that used in the physiological studies (Litovsky and Yin, 1993, 1994; Fitzpatrick *et al.*, 1995). Specifically, the number of spikes in response to each click was counted in a window with a fixed duration, which was determined by the observation of the PST histogram or dot-raster plot. (If the windows for the leading and lagging stimuli overlapped, the number of spikes in response to the leading stimulus was set to the average number of spikes when the stimulus was given alone. Then, the number of spikes in response to the lagging click was calculated by subtracting this average number from the total number of spikes in the overlapping window.)

1. Leading stimulus with strong ITD more suppressive

The model IC neuron received inputs from the ipsilateral and contralateral MSO model neurons with both CDs equal to zero. Detailed parameters of the IC and MSO model neurons in this case are listed in Table V. The excitatory input parameters of the IC model were identical to those described

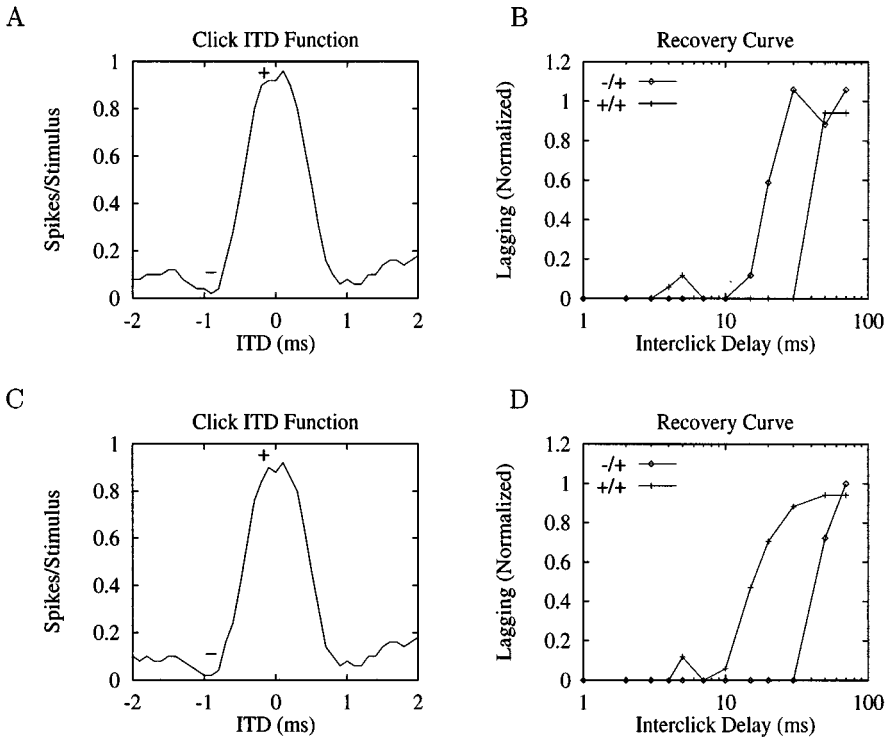

FIG. 10. Response of two model IC neurons to pairs of binaural clicks. For the model neuron with responses shown in upper panels (parameters are given in Table V), a leading stimulus with an ITD that elicited a strong response (a strong ITD) was more suppressive. For the model neuron with responses shown in lower panels (parameters are given in Table VI), a leading stimulus with an ITD that elicited a weak response (a weak ITD) was more suppressive. (A) and (C) click ITD functions. The plus sign (''+'') indicates the strong ITD (0 μs) and the minus sign (''−'') indicates the weak ITD (−900 μs). Using these notations, conditions for paired binaural clicks are indicated in panels (B) and (D) as follows: ''+/+'' indicates that the strong ITD value (0 μs) was used for both the leading and the lagging clicks, and ''−/+'' indicates that the weak ITD (−900 μs) was used for the leading click and the strong ITD (0 μs) was used for the lagging click.

in Table I. The input parameters of the ipsilateral MSO neuron were chosen such that its ITD function showed a maximal response of approximately 1 spike/stimulus (at around zero ITD) and a minimal response of approximately no discharges (at an ITD of −900 μs). The parameters of the contralateral MSO neuron were chosen so that the response rates at 0 and 900 μs differed by at least 50%. Other choices of the parameters did not change the essential properties of the simulation results as long as the ITD sensitivities of the two MSO neurons were preserved.

The click ITD function of the IC model neuron in Fig. 10(A) shows a peak around zero ITD and troughs around +1 and −1 ms. The absence of peaks at ±2 ms was due to the inhibitions from onset cells to the ipsilateral MSO model neuron. Based on this ITD function, the strong ITD was chosen at zero and the weak ITD at −900 μs. As in physiological studies, in order to study the effects of the leading stimulus on the suppression of the response to the lagging stimulus, the lagging stimulus was always at the strong ITD of the cell whereas the leading ITD could be at either the strong or the weak ITD. The former case was represented by ''+/+'' and the latter case by ''−/+'' in Fig. 10.

The recovery curves in Fig. 10(B) illustrate the responses of the model neuron to lagging stimuli at various interclick delays for both ''+/+'' and ''−/+'' cases. The responses to lagging stimuli were normalized by dividing the number of discharges by the average number of discharges when the stimulus was delivered alone (Fitzpatrick *et al.*, 1995). In the ''+/+'' case, the response of the model neuron to the lagging click was suppressed for as long as 40 ms. In the ''−/+'' case, on the other hand, the response to the lagging click was recovered 15 ms after the leading click.

A comparison between the recovery curves of the model neuron [Fig. 10(B)] and real IC neurons indicated that the recovery of real neurons was more gradual. This difference may be due to the facts that the IC model neuron received only one inhibitory input and that this inhibition had a fixed synaptic strength and time constant. It is suggested that IC neurons may receive multiple inputs and/or that the amount of inhibitory neurotransmitter released varies from trial to trial.

2. Leading stimulus with a weak ITD more suppressive

To simulate the IC neurons for which a leading stimulus with a weak ITD was more suppressive, a different CD of the contralateral MSO model neuron was chosen. Detailed information on model parameters is given in Table VI. Note that the parameters for the ipsilateral MSO and IC model neurons were the same as in above simulation. The contralateral MSO neuron had a CD of 900 μs. Although this CD was out of the physiologically related ITD range for cats, this value was used simply to illustrate the possibility for prominent

TABLE VI. Parameters of an IC model neuron simulating ITD-dependent echo suppression. This neuron showed stronger suppression when the leading click had an ITD that elicited a weak response. Parameters shown in italics are those critical for the simulation of data. The dashes, —, represent ''not applicable.''

Parameters	Ipsilateral MSO		Contralateral MSO		IC	
	exc	inh	exc	inh	exc	inh
Number of projecting neurons	6(C,I)	6(C,I)	6(C,I)	6(C,I)	1(I)	1(C)
Synaptic strength (nS)	2.0	7.0	2.0	1	25	*30*
Time constant (ms)	0.1	4	0.1	2	0.1	*20*
CD of MSO (μs)	0		*900*		—	—
Delay of arrival (ms)	0	0	0	0	0	1

effects with parameters similar to those used for other simulations here. A MSO model neuron of CF of 1000 Hz with CD at 400 μs would have given a similar result.

Figure 10(C) shows the click ITD function of the model neuron. Since the inhibitory input to the IC was delayed by 1 ms, the inhibitory MSO model neuron did not affect the click ITD function of the IC at small interaural delays. Therefore the ITD function in Fig. 10(C) is identical to that in Fig. 10(A). As noted above, the strong ITD was chosen at zero and the weak ITD at -900 μs. The same stimuli were presented and the same methods were employed to generate and analyze the simulation results. The recovery curves are shown in Fig. 10(D). It is clear that this neuron showed the opposite result to that in Fig. 10(B). For this model neuron, the responses to the lagging stimulus in the ''$-/+$'' case were more strongly suppressed than those in ''$+/+$'' case. The suppression lasted tens of milliseconds even when the neuron did not respond to the leading stimulus. Like the model neuron with responses shown in the upper panels of Fig. 10, this model neuron recovered from the suppression more abruptly than real IC neurons.

III. DISCUSSION

The Hodgkin–Huxley type model for the IC neurons in this paper received an excitatory and an inhibitory input from MSO model neurons. This simple structure is not necessarily a realistic description of the anatomy; however, it has the ability to describe a variety of physiological data from the IC, including the responses to pure tones, binaural beat stimuli, interaural phase-modulated stimuli, single binaural clicks, and pairs of binaural clicks. An abstract model, which functionally simulates the excitatory and inhibitory effects of the inputs, would be able to give similar results. Physiological models seem to be more appropriate in this study based on the rationale for the modeling approach stated in the Introduction.

A. Responses to sustained stimuli

1. ITD sensitivities

The ITD sensitivity of IC neurons has been studied extensively. It was found that more than 80% of low-frequency IC neurons were sensitive to interaural delay (Yin and Kuwada, 1984). These neurons show cyclic responses at the stimulating frequency. Two types of ITD functions were generated in our simulations. One had only one maximum in a cycle and the other, more unusual, had two peaks in one cycle. The double-peaked ITD functions have been observed from IC neurons but have not been observed in MSO neurons (Yin, personal communication). These observations suggest that the bimodal function is associated with the convergence of auditory pathways on the IC.

Based on the simulation results, the shape of ITD functions depends on the interaction between the excitation and inhibition to the IC at given ITDs. Therefore the stimulus frequency or the CD of either of the MSO model neurons could affect the ITD sensitivity of the IC model neuron. The simulation of the ITD functions of IC model neurons at three different stimulus frequencies showed that an ITD function which was unimodal at some frequencies could be bimodal at other frequencies. Consistent with the model prediction, a neuron showing this property is illustrated in Yin and Kuwada (1983a, their Fig. 3, neuron 78145-3).

2. Characteristic delay and phase-frequency function

The concept of ''characteristic delay'' was introduced by Rose *et al.* (1966). They found that the ITD functions at different frequencies appeared to have a peak or trough at a common delay, which is referred to as the characteristic delay. In our simulations, ITD functions with a single peak could be obtained with either weak inhibition or strong inhibition from the contralateral MSO model neuron. In the case of weak or absent inhibition, the peak in the ITD function corresponds to the characteristic delay of the neuron, as in the MSO model neuron. In these cells, a common peak can be observed for different stimulus frequencies. In the case of strong inhibition, however, the peak in the ITD function may not correspond to a CD in this sense because the peak response may not happen at the same ITD for different stimulation frequencies. In this case, the minima occur at a common ITD. A response of this type in the IC might be interpreted as the result of excitatory-inhibitory inputs from the LSO; however, these modeling results indicate that the same response pattern can occur due to inhibition from the contralateral MSO.

A quantitative measurement of the CD was introduced by Yin and Kuwada (1983b). They explored the concept of characteristic delay in great detail both with physiological experiments and with computer simulations. They plotted the mean interaural phase of the response against the stimulating frequency and found that for the 201 runs on 82 phase-sensitive IC neurons, about 60% were identified as having a

CD at an acceptable significance level, meaning that the relationship of phase and frequency is linear.

If phase-frequency functions of IC model neurons in this study were plotted with a denser sampling frequency, we believe that both linear and nonlinear functions would result. When the inhibition from the contralateral MSO model neuron was weak or absent, the response of the IC model neuron basically followed that of the ipsilateral MSO model neuron and showed a linear phase-frequency plot for the frequencies near its CF. When the inhibition from the contralateral MSO was strong enough to affect the ITD-tuning of the IC, the phase-frequency function was not generally linear, since there was no common peak for these ITD functions. The peak of the ITD function of the IC model neuron depended not only on the stimulus frequency but also on the interaction between two MSO model neurons. Consistent with this prediction, neuron 79151-6 in Fig. 6 of Yin and Kuwada (1983b) showed bimodal ITD functions at several stimulus frequencies and its phase-frequency function was nonlinear.

3. Phase locking

Phase locking is an important feature for neurons responsible for ITD encoding. Although many low-frequency IC neurons are sensitive to interaural delay, only a small percent of them phase lock to monaural stimuli [about 18% in 82 neurons in Yin and Kuwada (1984)]. For those which do phase lock, the synchronization index is low. The synchronization index of the IC model neuron to monaural stimuli showed a slight decrease relative to that of the MSO model neurons. The slight decrease in the degree of phase locking resulted partly from the inhibitory input to the IC model neurons. The decrease of the synchronization index was proportional to the strength of inhibition. Since the inhibition to the IC was not perfectly phase locked, it made the membrane potential more random. Hence the inhibition not only changed the probability of firing at a certain time, but also changed the exact time of firing of the neuron.

A possible mechanism for the decrease of phase locking in actual IC neurons is that IC neurons receive multiple inputs. A cell that is driven by several inputs which are phase locked to different phases will be phase locked at a lower degree than each of its inputs. In addition, the phase locking of the model cell is also influenced by its membrane properties. In any case, it is clear that the current model with only one excitatory and one inhibitory input cannot describe the dramatic decrease in phase locking of the IC.

4. Sensitivity to dynamic temporal features

In binaural beat stimuli and interaural phase-modulated tones, the interaural time differences change as a function of time. The sensitivity of IC neurons to these dynamic temporal features was first systematically studied by Spitzer and Semple (1993). The nonoverlapping IPD arcs in response to IPM stimuli are consistent with the binaural beat data of the IC (Yin and Kuwada, 1983a; Spitzer and Semple, 1991), which showed the sharpening effect of a dynamically elicited response. Spitzer and Semple used the same time-varying IPD stimuli on gerbil SOC neurons and found that for most units the responses to IPM stimuli were overlapping for overlapping IPD ranges (Spitzer and Semple, 1992). Their results suggest that the SOC initially encodes instantaneous IPD, while further processing in the IC provides the dependence on the time course of IPD.

In the IC model presented in this paper, there was no mechanism incorporated that was influenced by the history of the response. It is not surprising that the current model does not describe the nonoverlapping IPD arcs in response to IPM stimuli. An extension of this model with an adaptation mechanism, presented in the accompanying paper, is able to describe the effects of dynamic phase (Cai *et al.*, 1997).

B. Responses to transient stimuli

1. Gradualness of recovery

When pairs of binaural clicks are presented at short interstimulus delays, the number of discharges of IC neurons evoked by the lagging stimulus is smaller than that evoked by the lagging stimulus alone. As the interclick delay gets longer, the response to the lagging stimulus recovers (Litovsky and Yin, 1993, 1994; Fitzpatrick *et al.*, 1995). The recovery can be also observed in the responses to single binaural clicks at a large ITD (Carney and Yin, 1989). The comparison of the recovery of IC neurons with that of the model neuron indicated that the recovery of real neurons is more gradual than that of the model neuron. This observation suggests that a single IC neuron receives inhibition from multiple sources. Since the stellate cells in the IC have dendrites extended across the fibrodendritic laminae, each of them may receive inputs from more than one population of synaptic endings (Oliver and Morest, 1984). Even though the dendritic field of disk-shaped cells is confined in a very narrow range (about 50 μm), these cells also receive large numbers of synaptic inputs on both dendrites and, in some cases, cell bodies (Oliver and Morest, 1984; Oliver, 1987; Shneiderman and Oliver, 1989). In addition, most, if not all, IC neurons send collaterals to nearby neurons (Oliver and Huerta, 1992). The effects of these synaptic inputs are not clear; however, they may affect the response of IC neurons, including the recovery to the lagging stimulus.

2. Onset inhibition to the IC

We found that the inhibitory inputs to the IC model in the simulation of the responses to sustained stimuli had to be much weaker to describe the data than those in the simulation of the responses to transient stimuli. If the parameters of the inhibition from the contralateral MSO were made strong enough to cause tens of milliseconds of silence of the model neuron at stimulus onset, the sustained response of the model neuron to a long-duration tone would be eliminated. The same issue has been discussed in Brughera *et al.* (1996). The coexistence of strong inhibition at stimulus onset and sustained response to an ongoing stimulus (Carney and Yin, 1989) indicates that IC neurons may receive strong onset inhibition in addition to the sustained inhibition. Many IC neurons with onset inhibition were reported in Kuwada *et al.* (1989).

There are several possible causes for this phenomenon. First, IC neurons may receive onset inhibition in addition to the inhibition from DNLL. This inhibition may come from monaural nuclei or interneurons inside the IC. The projections from the VNLL to the IC are apparently glycinergic, suggesting that cells in the VNLL act as inhibitory interneurons between the octopus cells in the cochlear nucleus and the IC (Adams and Wenthold, 1987). It is possible that IC neurons receive onset inhibition from octopus cells directly via VNLL (Adams and Wenthold, 1987). Second, the DNLL may not be a faithful relay of the MSO on its ipsilateral side. Some neurons in the DNLL responded to binaural tones with only onset responses or onset responses followed by weak sustained responses (Brugge *et al.*, 1970) depending on interaural disparities. Third, some neurons in the contralateral MSO might be onset cells. The lack of any report of onset cells in the MSO might be related to the lack of recording of the responses of MSO neurons to transient stimuli, which is due to the strong field potential within the MSO (Guinan *et al.*, 1972). Further physiological experiments are needed to clarify these possibilities.

C. Comparisons with other models

1. Comparison with the MSO model

Since the IC model in this study incorporated MSO models to provide inputs, the responses of the MSO model neurons to each stimulus were obtained. Therefore it was convenient to compare the MSO model and the IC model in this study.

The MSO model showed a cyclic ITD function when a pure-tone stimulus was presented. In response to binaural click stimuli, the MSO model cell with inhibitory inputs also showed early and/or late inhibition. The asymmetry of responses with positive and negative interaural delay depended on the asymmetry of the inhibitory inputs to the neuron. The single MSO cell model did not show bimodal ITD functions, direction and rate sensitivities, ITD-dependent echo suppression, and sharpened dynamic IPD functions. Therefore it was not adequate as a model for cells in the IC.

The IC model presented in this paper was consistent with a larger set of observed IC behavior. In addition to properties demonstrated by the MSO model, it showed bimodal IPD functions with some choices of the inhibitory parameters from the contralateral MSO. It also showed sensitivity to the direction and the speed of the binaural beat stimulus, when the contralateral inhibition lasted for a long time (tens of milliseconds). In response to pairs of binaural clicks, the model neuron showed ITD-dependent echo suppression. This ITD-dependence was determined by the characteristic delay of the inhibitory MSO model neuron.

Neither of these models described the gradual recovery of the response to a lagging transient stimulus when two stimuli are applied one after another with a short delay. It was suggested that this gradual recovery may reflect the fact that IC neurons may receive multiple inhibitory and excitatory inputs. The variability of the synaptic characteristics and the response probability of these sources might also contribute to the gradual recovery. The model did not show the coexistence of strong onset inhibition and sustained responses to long-duration stimuli, unless inhibitory inputs were provided to the IC by onset neurons. [See the related discussion by Brughera *et al.* (1996).] Finally, this IC model did not show sharpened dynamic IPD functions.

2. Comparison with a functional model with lateral inhibition

Besides the physiological models developed for the IC, functional models for psychophysics (such as cross-correlation models) have been developed for several decades (see the review by Colburn, 1996). Among those models, the Lindemann (1986a, b) model incorporated a dynamic lateral inhibition mechanism and monaural channels that provided inputs to the interaural cross-correlation function. These extensions allow the model to provide a basis for the precedence effect. When there are coincidences at one value of ITD, the model generates inhibitions to the coincidences at other values of ITD. Hence the Lindemann model predicts that minimum echo suppression happens when the leading stimulus and lagging stimulus come from the same location and maximum suppression happens when the leading stimulus and lagging stimulus are lateral to each other in space. Psychophysical evidence also suggests (on the basis of very little data) (Boerger, 1965) that echo suppression is stronger when sources are widely separated. This relationship only partially describes the data observed in physiology (Litovsky and Yin, 1993, 1994; Fitzpatrick *et al.*, 1995). The Lindemann model cannot predict the data in which suppression can be strongest when both the leading and lagging stimuli come from the same source. The physiological model described in this paper with excitation and inhibition coming from independent sources described both psychophysical and physiological data.

IV. CONCLUSIONS

Simulation results revealed that the IC model with ipsilateral excitation and contralateral inhibition from ITD-sensitive neurons showed unimodal and bimodal ITD functions, rate and direction sensitivities to binaural beat stimuli, early and late inhibition in response to binaural clicks, and ITD-dependent echo suppression in response to pairs of binaural clicks. With the current model structure and membrane function, the model did not show sensitivity to dynamic temporal features or sharpened dynamic IPD functions in response to binaural beat stimuli and interaural phase-modulated stimuli. It also did not show gradual recovery curves in response to transient stimuli and the dramatic decrease of phase locking to monaural tone stimuli. In order to show some of these features, mechanisms such as adaptation (Cai *et al.*, 1997) and a more complex model structure were needed.

ACKNOWLEDGMENTS

This work was supported by NIH Grant No. R01-DC00100 (H.S.C.) and NIH Grant No. R29-DC01641 (L.H.C.) from the National Institute of Deafness and other Communication Disorders, NIH.

Adams, J. C., and Mugnaini, E. (**1984**). ''Dorsal neucleus of lateral lemniscus: A nucleus of GABAergic projection neurons,'' Brain Res. Bull. **13**, 585–590.

Adams, J. C., and Wenthold, R. J. (**1987**). ''Immunostaining of ascending auditory pathways with glycine antiserum,'' Assoc. Res. Otolaryngol. **10**, 63.

Blauert, J. (**1983**). ''The psychophysics of human sound localization,'' in *Spatical Hearing* (MIT, Cambridge, MA), pp. 1–408.

Boerger, G. (**1965**). ''Über die Trägheit des Gehörs bei der Richtungsempfindung [On the persistence of the directional sensation in hearing],'' *Proceedings of the 5th International Congress on Acoustics*, liége, B 27.

Brugge, J. F., Anderson, D. J., and Aitkin, L. M. (**1970**). ''Responses of neurons in the dorsal nucleus of lateral lemniscus of cat to binaural tonal stimulation,'' J. Neurophysiol. **33**, 441–458.

Brughera, A. R., Stutman, E. R., Carney, L. H., and Colburn, H. S. (**1996**). ''A model with excitation and inhibition for cells in the medial superior olive,'' Aud. Neurosci. **2**, 219–233.

Cai, H. (unpublished).

Cai, H. (**1997**). ''Models for the binaural response properties of inferior colliculus neurons,'' dissertation, Boston University.

Cai, H., Carney, L. H., and Colburn, H. S. (**1998**). ''A model for binaural response properties of inferior colliculus neurons: II. A model with interaural time difference sensitive excitatory and inhibitory inputs and an adaptation mechanism,'' J. Acoust. Soc. Am. **103**, 494–506.

Cant, N. B., and Hyson, R. L. (**1992**). ''Projections from the lateral nucleus of the trapezoid body to the medial superior olivary nucleus in the gerbil,'' Hearing Res. **49**, 281–298.

Carney, L. H. (**1993**). ''A model for the responses of low-frequency auditory-nerve fibers in cat,'' J. Acoust. Soc. Am. **93**, 401–417.

Carney, L. H., and Yin, T. C. T. (**1989**). ''Responses of low-frequency cells in the inferior colliculus to interaural time differences of clicks: Excitatory and inhibitory components,'' J. Neurophysiol. **62**, 144–161.

Colburn, H. S. (**1996**). ''Computational models of binaural processing,'' in *Auditory Computation*, edited by H. Hawkins and T. McMullen (Springer-Verlag, Berlin), pp. 332–400.

Colburn, H. S., and Ibrahim, H. (**1993**). ''Modeling of precedence effect behavior in single neurons and in human listeners,'' J. Acoust. Soc. Am. **93**, 2293(A).

Eccles, J. C. (**1964**). *The Physiology of Synapses* (Academic, New York).

Finlayson, P. G., and Caspary, D. M. (**1989**). ''Synaptic potentials of chinchilla lateral superior olivary neurons,'' Hearing Res. **38**, 221–228.

Fitzpatrick, D. C., Kuwada, S., Batra, R., and Trahiotis, C. (**1995**). ''Neural responses to simple simulated echoes in the auditory brain stem of the unanesthetized rabbit,'' J. Neurophysiol. **74**, 2469–2486.

Glendenning, K. K., Brunso-Bechtold, J. K., Thompson, G. C., and Masterton, R. B. (**1981**). ''Ascending auditory afferents to the nuclei of the lateral lemniscus,'' J. Comp. Neurol. **197**, 673–703.

Goldberg, J. M., and Brown, P. B. (**1969**). ''Response of binaural neurons of dog superior olivary complex to dichotic tonal stimuli: some physiological mechanisms for sound localization,'' J. Neurophysiol. **32**, 613–636.

Guinan, Jr., J. J., Norris, B. E., and Guinan, S. S. (**1972**). ''Single auditory units in the superior olivary complex. II. Locations of unit categories and tonotopic organization,'' Int. J. Neurosci. **4**, 147–166.

Henkel, C. K., and Spangler, K. M. (**1983**). ''Organization of the efferent projections of the MSO nucleus in the cat as revealed by HRP and autoradiographic tracing methods,'' J. Comp. Neurol. **221**, 416–428.

Hodgkin, A. L., and Huxley, A. F. (**1952**). ''A quantitative description of membrane current and its application to conduction and excitation in the nerve,'' J. Physiol. (London) **117**, 500–544.

Johnson, D. H. (**1980**). ''The relationship between spike rate and synchrony in responses of auditory-nerve fibers to single tones,'' J. Acoust. Soc. Am. **68**, 1115–1122.

Joris, P. X., Carney, L. H., Smith, P. H., and Yin, T. C. T. (**1994**). ''Enhancement of neural synchronization in the anteroventral cochlear nucleus. I. Responses to tones at the characteristic frequency,'' J. Neurophysiol. **71**, 1022–1036.

Kuwada, S., Batra, R., and Fitzpatrick, D. C. (**1997**). ''Neural processing of binaural temporal cues,'' in *Binaural and Spatial Hearing in Real and Virtual Environments*, edited by R. H. Gilkey and T. R. Anderson (Erlbaum, Mahwah, NJ), pp. 399–426.

Kuwada, S., Batra, R., and Stanford, T. R. (**1989**). ''Monaural and binaural response properties of neurons in the inferior colliculus of the rabbit: Effects of sodium pentobarbital,'' J. Neurophysiol. **61**, 269–282.

Kuwada, S., Stanford, T. R., and Batra, R. (**1987**). ''Interaural phase-sensitive units in the inferior colliculus of the unanesthetized rabbit: Effects of changing frequency,'' J. Neurophysiol. **57**, 1338–1360.

Kuwada, S., and Yin, T. C. T. (**1983**). ''Binaural interaction in low-frequency neurons in inferior colliculus of the cat. I. Effects of long interaural delays, intensity, and repetition rate on interaural delay function,'' J. Neurophysiol. **50**, 981–999.

Kuwada, S., Yin, T. C. T., Syka, J., Buunen, T. J. F., and Wickesberg, R. E. (**1984**). ''Binaural interaction in low-frequency neurons in inferior colliculus of the cat. IV. Comparison of monaural and binaural response properties,'' J. Neurophysiol. **51**, 1306–1325.

Lindemann, W. (**1986a**). ''Extension of a binaural cross-correlation model by contralateral inhibition. I. Simulation of lateralization for stationary signals,'' J. Acoust. Soc. Am. **80**, 1608–1622.

Lindemann, W. (**1986b**). ''Extension of a binaural cross-correlation model by contralateral inhibition. II. The law of the first wave front,'' J. Acoust. Soc. Am. **80**, 1623–1630.

Litovsky R., and Yin, T. C. T. (**1993**). ''Single-unit responses to stimuli that mimic the precedence effect in the inferior colliculus of the cat.'' Assoc. Res. Otolaryngol. Abstr. **16**, 128.

Litovsky, R., and Yin, T. C. T. (**1994**). ''Physiological correlates of the precedence effect: Free field recordings in the inferior colliculus of the cat,'' Assoc. Res. Otolaryngol. Abstr. **17**, 337.

Manis, P. B., and Marx, S. O. (**1991**). ''Outward currents in isolated ventral cochlear nucleus neurons,'' J. Neurosci. **11**, 2865–2880.

Mardia, K. V. (**1972**). *Statistics of Directional Data* (Academic, London).

Oertel, D. (**1983**). ''Synaptic responses and electrical properties of cells in brain slices of the mouse anteroventral cochlear nucleus,'' J. Neurosci. **3**, 2043–2053.

Oertel, D. (**1985**). ''Use of brain slices in the study of the auditory system: spatial and temporal summation of synaptic inputs in cells in the anteroventral cochlear nucleus of the mouse,'' J. Acoust. Soc. Am. **78**, 328–333.

Oliver, D. L. (**1987**). ''Projections to the inferior colliculus from the anteroventral cochlear nucleus in the cat: possible substrates for binaural interaction,'' J. Comp. Neurol. **264**, 24–46.

Oliver, D. L., and Huerta, M. F. (**1992**). ''Inferior and superior colliculus,'' in *The Mammalian Auditory Pathway: Neuroanatomy*, edited by D. B. Webster, A. N. Popper, and R. R. Fay (Springer-Verlag, Berlin), pp. 168–221.

Oliver, D. L., and Morest, D. K. (**1984**). ''The central nucleus of the inferior colliculus in the cat,'' J. Comp. Neurol. **222**, 237–264.

Peruzzi, D., and Oliver, D. L. (**1995**). ''Intrinsic membrane properties and morphology of neurons in the rat inferior colliculus,'' Assoc. Res. Otolaryngol. Abstr. **18**, 515.

Rose, J. E., Gross, N. B., Geisler, C. D., and Hind, J. E. (**1966**). ''Some neural mechanisms in the inferior colliculus of the cat which may be relevant to localization of a sound source,'' J. Neurophysiol. **29**, 288–314.

Rothman, S. R., Young, E. D., and Manis, P. B. (**1993**). ''Convergence of auditory nerve fibers onto bushy cells in the ventral cochlear nucleus: implications of a computational model,'' J. Neurophysiol. **70**, 2562–2583.

Shneiderman, A., Chase, M. B., Rockwood, J. M., Benson, C. G., and Potashner, S. J. (**1993**). ''Evidence for a GABAergic projection from the dorsal nucleus of the lateral lemniscus to the inferior colliculus,'' J. Neurochem. **60**, 72–82.

Shneiderman, A., and Oliver, D. L. (**1989**). ''EM autoradiographic study of the projections from the dorsal nucleus of the lateral lemniscus: A possible source of inhibitory inputs to the inferior colliculus,'' J. Comp. Neurol. **286**, 28–47.

Shneiderman, A., Oliver, D. L., and Henkel, C. K. (**1988**). ''Connections of the dorsal nucleus of the lateral lemniscus: An inhibitory parallel pathway in the ascending auditory system?,'' J. Comp. Neurol. **276**, 188–208.

Smith, P. H. (**1995**). ''Structural and functional differences distinguish principal from non-principal cells in the guinea pig MSO slice,'' J. Neurophysiol. **73**, 1653–1667.

Smith, P. H., Joris, P. X., and Carney, L. H. (**1991**). ''Projections of physiologically characterized globular bushy cell axons from the cochlear nucleus of cat,'' J. Comp. Neurol. **304**, 387–401.

Smith, P. H., and Rhode, W. S. (**1987**). ''Characterization of HRP-labeled globular bushy cells in the cat anteroventral cochlear nucleus,'' J. Comp. Neurol. **266**, 360–375.

Spitzer, M. W., and Semple, M. N. (**1991**). ''Interaural phase coding in auditory midbrain: influence of dynamic stimulus features,'' Science **254**, 721–724.

Spitzer, M. W., and Semple, M. N. (**1992**). ''Responses to time-varying

phase disparity in gerbil superior olive: evidence for hierarchical processing,'' Soc. Neurosci. Abstr. **18**, 149.
Spitzer, M. W., and Semple, M. N. (**1993**). ''Responses of inferior colliculus neurons to time-varying interaural phase disparity: effects of shifting the locus of virtual motion,'' J. Neurophysiol. **69**, 1245–1263.
Sujaku, Y., Kuwada, S., and Yin, T. C. T. (**1981**). ''Binaural interaction in the cat inferior colliculus: comparison of the physiological data with a computer simulated model,'' in *Neuronal Mechanisms of Hearing*, edited by J. Syka and L. Aitkin (Plenum, New York), pp. 233–238.
Wu, S. H., and Oertel, D. (**1984**). ''Intracellular injection with horseradish peroxidase of physiologically characterized stellate and bushy cells in slices of mouse anteroventral cochlear nucleus,'' J. Neurosci. **4**, 1577–1588.
Yin, T. C. T. (personal communication).
Yin, T. C. T. (**1994**). ''Physiological correlates of the precedence effect and summing localization in the inferior colliculus of the cat,'' J. Neurosci. **14**, 5170–5186.
Yin, T. C. T., and Chan, J. C. K. (**1990**). ''Interaural time sensitivity in medial superior olive of cat,'' J. Neurophysiol. **64**, 465–488.
Yin, T. C. T., Chan, J. C. K., and Carney, L. H. (**1987**). ''Effects of interaural time delays of noise stimuli on low-frequency cells in the cat's inferior colliculus. III. Evidence for cross-correlation,'' J. Neurophysiol. **58**, 562–583.
Yin, T. C. T., Chan, J. C. K., and Irvine, D. R. F. (**1986**). ''Effects of interaural time delays of noise stimuli on low-frequency cells in the cat's inferior colliculus. I. Responses to wideband noise,'' J. Neurophysiol. **55**, 280–300.
Yin, T. C. T., and Kuwada, S. (**1983a**). ''Binaural interaction in low-frequency neurons in inferior colliculus of the cat. II. Effects of changing rate and direction of interaural phase,'' J. Neurophysiol. **50**, 1000–1019.
Yin, T. C. T., and Kuwada, S. (**1983b**). ''Binaural interaction in low-frequency neurons in inferior colliculus of the cat. III. Effects of changing frequency,'' J. Neurophysiol. **50**, 1020–1042.
Yin, T. C. T., and Kuwada, S. (**1984**). ''Neuronal Mechanisms of Binaural Interaction,'' in *Dynamic Aspects of Neocortical Function*, edited by G. M. Edelman, W. E. Gall, and W. M. Cowan (Wiley, New York), pp. 263–313.